

Integration Technologies for a Fully Modular and Hot-Swappable MV Multi-Level Concept Converter

Didier Cottet, Wim van der Merwe, Francesco Agostini, Gernot Riedel, Nikolaos Oikonomou, Andrea Rüetschi, Tobias Geyer, Thomas Gradinger, Rudi Velthuis, Bernhard Wunsch, David Baumann, Willi Gerig, Franz Wildner, Vinoth Sundaramoorthy, Enea Bianda, Franz Zurfluh, Richard Bloch, Daniele Angelosante, Dacfey Dzung, ABB Switzerland Ltd., Corporate Research, 5405 Baden-Dättwil, Switzerland

Tormod Wien, Anne Elisabeth Vallestad, Dalimir Orfanus, Reidar Indergaard, Harald Vefling, Arne Heggelund, ABB Norway Ltd., Corporate Research, 1375 Billingstad, Norway

Jonathan Bradshaw, DPS Ltd., Auckland 1010, New Zealand

Contact: didier.cottet@ch.abb.com

Abstract

In order to fully exploit the benefits of modular converters, dedicated hard- and software integration technologies have been developed to complement modular multi-level circuit topologies. The technologies investigated include a wireless auxiliary power supply, a two-phase cooling, solid insulation, wireless optical communication, redundant EtherCAT networking and advanced IGBT junction temperature diagnostics. Emphasis was set on three key aspects of modularity: *scalability*, *configurability* and *pluggability*. To validate the technologies and to demonstrate their benefits, a medium voltage concept converter was built and operated. The combination of these technologies finally also enabled a ‘hot swap’ functionality, where power modules can be replaced during converter operation. Hot swap has successfully been tested for a DC-link voltage of 3.3 kV and output power of 550 kW.

1. Introduction

Modular converters are typically motivated by electrical properties, such as paralleling and series connection for power and voltage scaling and series connection for converter voltages higher than the semiconductors’ blocking voltages. Furthermore, modular multi-level topologies are used to increase power quality and efficiency. Complementary to these aspects, this paper focuses on the modularity of specific integration technologies, including auxiliary power supply, cooling, electrical insulation, and software and hardware components associated with the control communication and IGBT junction temperature diagnostic.

In order to define the requirements for the investigated technologies, three different aspects of *modularity* must be evaluated: *scalability*, *configurability* and *pluggability* (see [1], [2] and [3] for further information on modularity). Which one of the three aspects is more relevant is motivated by the specific business case underlying a converter development, which can include: converter variants deployment for a broad product range, higher production volumes of fewer parts to take advantage of economy of scale factors, assembly and commissioning, testing, servicing, reliability and lifetime (availability). Finally, it is expected that the combination of modular topologies with modular integration brings additional benefits, one of which is ‘hot swap’, the capability of replacing power modules during full operation.

In this work, a modular multi-level topology based (MMC) [4] concept converter is used, around which the integration technologies have been developed. The MMC topology by itself and its control algorithm are not scope of this paper. In Section 2, the individual technologies are described and brought into context with each other. Section 3 presents the full scale, medium voltage concept converter that was built to demonstrate the developed technologies.

2. Technologies

The power electronic building blocks (PEBBs, see Figure 1b) address the challenges of configurability and scalability as the internal unipolar cells can be connected as series, parallel or full-bridge configuration for various applications and power requirements. The PEBBs can then be series connected to reach the required converter voltages. In the present demonstrator converter (Figure 1a), the cells are rated for a maximum of 1 kV and 600 A.

An additional requirement is that of voltage insulation capable of handling the increasing system-level voltage, the independent PEBB cooling, the system communication with variable number of cells and the reliability which is reduced with the increasing part count.

Finally, the PEEBs need to be pluggable to allow fast assembly, commissioning and servicing of the converter. This pluggability must be provided by the converter cabinets as well as by all power and auxiliary interfaces.



Figure 1: Photographs of the concept converter (a) and of the PEBB containing two unipolar cells (b).

2.1. Wireless Auxiliary Power Supply

In MMC topologies, the individual power modules (power cells) can be self-powered from the cell's capacitor voltage. This, however, requires the application of main power to charge the cell capacitors above a certain threshold before the cell logic turns on. This dependency brings several disadvantages with regard to commissioning, maintenance and hot swap. For this reason, a wireless, inductive power transfer (IPT) based solution was developed [5]. The IPT system consists of a resonant DC-AC-DC converter with a pair of coupled coils L_1 and L_2 acting as resonant tank with series connected compensating capacitors C_1 and C_2 [6] (Figure 2a). The coupled coils also provide the pluggability and the galvanic insulation. The IPT system was designed for a power supply of 30 W with an input voltage of 48 V_{DC}, an output voltage to the cells of 27 V_{DC} ±4 V and aimed at robustness and low cost rather than efficiency.

Two important boundary conditions had to be taken into account. First, the coupled coils have to work in an electrically conductive environment (PEBB enclosures, cabinet walls, bus bars, etc.), thus requiring a compact design which is insensitive to stray couplings of the magnetic field. Second, the coils are mounted inside the cooling air duct, and must not block the air flow. The chosen coil design therefore consist of an outer primary coil and an inner, concentric secondary coil, wound on a magnetic core to concentrate the magnetic flux (Figure 2b). In order to keep the system cost low, active regulation or per-part tuning are not permitted. The IPT system is therefore not operating at resonant frequency, since there the voltage gain is strongly load dependent and would need a regulator. Instead, a specific operation frequency is chosen, where the system can be designed for minimal load dependency [7]. Figure 3 shows the achieved efficiency of about 90 % (incl. inverter and rectifier) and the resulting load dependencies.

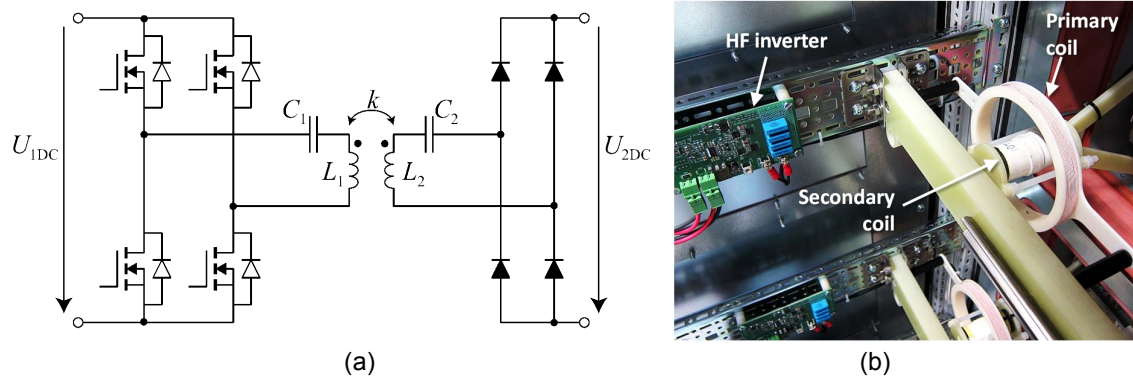


Figure 2: Resonant converter circuit (a), and photo of actual inverter PCB and coupled coils (b).

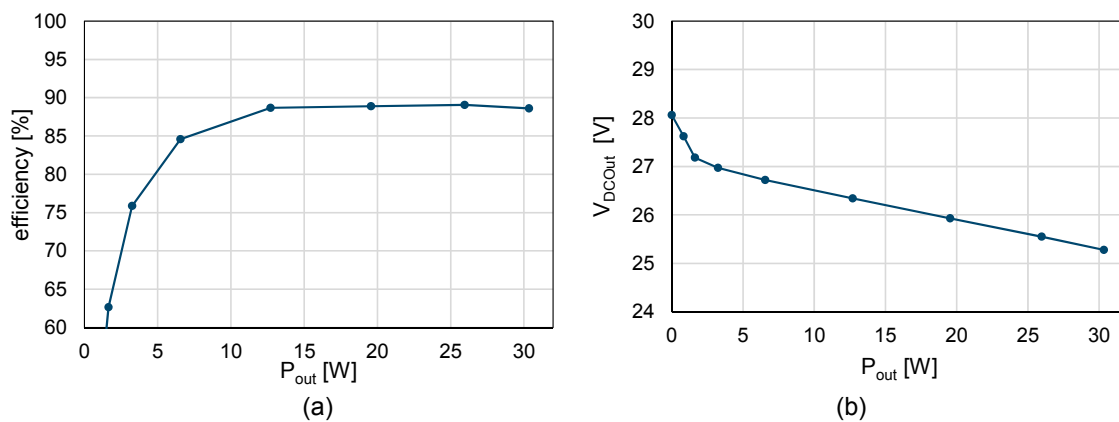


Figure 3: Measured efficiency (a) and output voltages (b) as function of output power.

2.2. Two-Phase Cooling

Air cooled converters based on finned heat sinks typically have lower power densities than water cooled converters. However, the piping required to water-cool the converter modules brings several disadvantages with regard to the pluggability of a modular system (i.e. need for pluggable dry connectors, electrically insulated pipes etc.). The solution chosen is therefore to use a local two-phase cooler for each power module and an air cooling system at cabinet level. The advantage of the two-phase approach is that it provides high cooling performance at small size and with low pressure losses [8]. In order to make best use of the available volume and air flow cross section, a dedicated L-shaped thermosyphon cooler has been developed (see Figure 4a). A horizontal evaporator variant and a vertical evaporator variant were implemented and benchmarked [9, 10 and 11]. For the final demonstrator, the vertical evaporator solution was chosen due to its higher cooling performance (Figure 4b). This cooling concept requires that the air flow through the cell and especially at the cell outlet after the condenser is not blocked by other components (i.e. auxiliary power supply coils).

The achieved performance is shown in Figure 5. For a volumetric air flow of 400 m³/h, air inlet temperature of 42 °C, maximum outlet temperature of 60 °C and maximum junction temperature of 125 °C, the achieved maximum cooling power is 1400 W. The pressure drop through the condenser at the same operating point is as low as 100 Pa which is up to an order of magnitude less than a comparable standard heat sink.

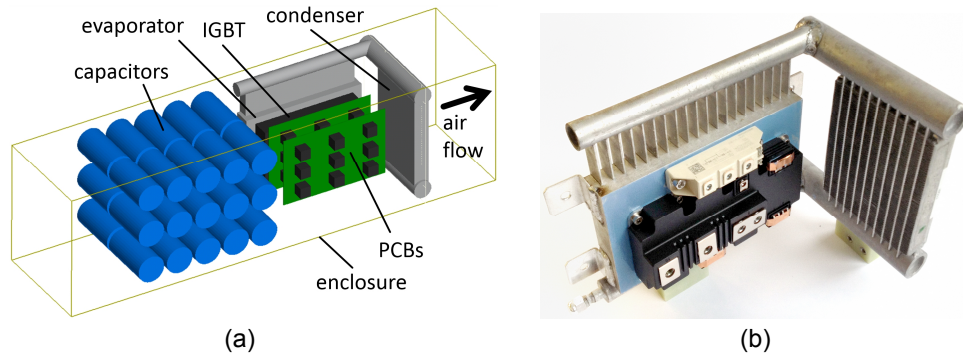


Figure 4: Cell cooling concept with air flow through capacitors, gate driver PCBs and thermosyphon condenser (a). Photo of actual cooler with mounted power semiconductor modules (b).

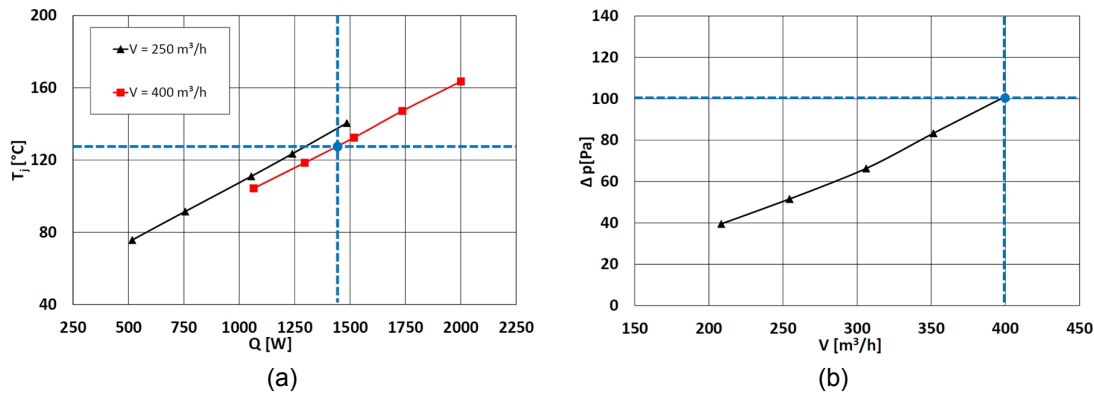


Figure 5: Measured IGBT junction temperature (a) and pressure drop (b).

2.3. Solid Insulation of Power Modules

One of the main advantages of the MMC topology is its capability to go to medium and high voltages, but to do so, the converter design must provide the necessary electrical insulation. Air insulation is, for many reasons, still the most widely used solution and it does not require any additional material. The drawback is that clearance and creepage distances rapidly increase with voltage and that the mechanical fixtures (e.g. inclusion of support insulators etc.) can become complex at higher voltages. In this work, a solid insulation based module enclosure was developed with the following motivation: volume reduction, explosion protection and easier mechanical handling. The known challenges are the attainment of partial discharge free dielectric material quality out of one piece (no bond lines) and to manufacture rounded part shapes for nearly homogenous E-fields [12].

The enclosure concept is such that the dielectric insulation is provided to the lateral and vertical directions, and air insulation is used in the front and rear of the module for the cooling air inlet and outlet. The manufacturing method consists of casting polyurethane (PU) material directly into pre-treated metal shells that are then kept as the inner and outer metallizations. This way, the dielectric material and the dielectric-to-metal interfaces provide the required quality. Figure 6 shows the manufacturing process and the resulting enclosure after machining. For technology demonstration purposes, the implemented enclosures were designed for 24 kV system voltage and 75 kV impulse voltage (overvoltage category II). The dielectric material showed excellent insulation properties with an E-field strength of 16 kV/mm at partial discharge extinction and no dielectric breakdown at 75 kV [13]. Electric breakdown was initialized in the air at the metallization edges. This can be further improved by more refined field grading.

The result is a PEBB enclosure with an outer metallization at ground potential, which brings many advantages such as: 1) direct galvanic mounting to fixtures and rail systems within the grounded cabinet racks, 2) full flexibility in positioning of the PEBBs where adjacent PEBBs can touch each other for maximum space saving, and 3) easy PEBB handling during hot swap.

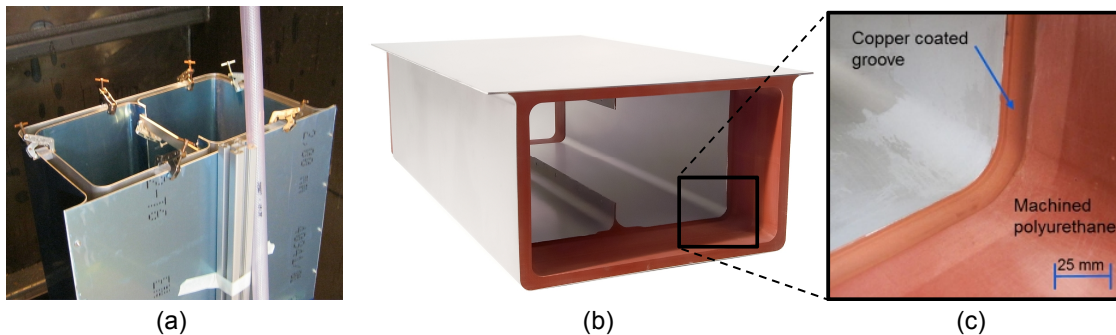


Figure 6: PU casting process (a) and actual enclosure (b) with detail of machined and copper coated E-field forming groove(c).

2.4. Two-Tier EtherCAT Based Communication Network

The two-tier communication network developed consists of a Xilinx Zynq based central controller connected to an EtherCAT (EC) network with free space optical infrared (IR) links (Figure 7). The first tier includes the time synchronized and redundant EC ring that distributes the control information to the EC slaves. From there, the second tier distributes the signals in star configuration via the free space optical (FSO) IR links to each MMC cell. The number of slaves per EC ring and the number of FSO links per EC slave can be freely configured, depending on the number of modules and required communication cycle time and synchronization jitter. The EC master was designed to be modular; support ring redundancy and clock synchronization [14], introduce minimal stack processing latency and run on different hardware platforms. Earlier implementations used a P2020 based main controller [15]. At present a Xilinx Zynq system-on-chip is used. A minimal bus cycle time of 11 μ s is achieved, now believed to be the fastest known in industry. Such low cycle times allow the accommodation of more EC slaves within 100 μ s control application cycle time.

The FSO links consist of two paralleled transmitting IR diodes with a total power of 2 x 100 mW peak and radiating in a ± 10 degrees wide beam, and one receiving photodiode, which works down to IR light levels of about 100 μ W/cm² (Figure 8a). Each link provides a raw data rate of 25 Mbit/s and a usable rate of 20 Mbit/s.

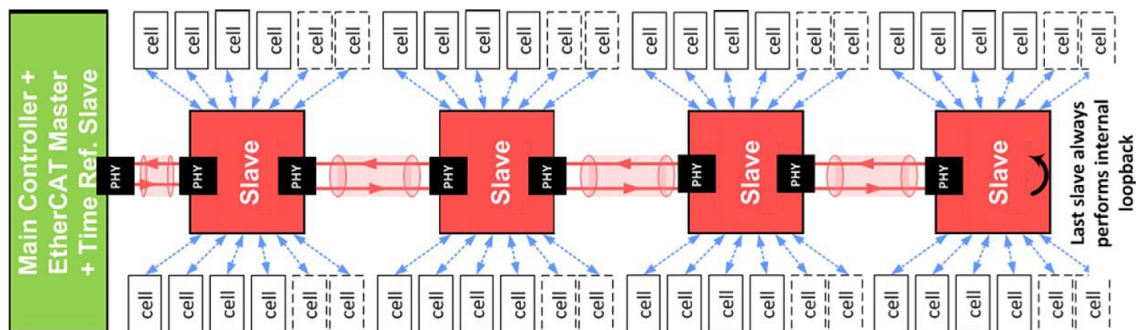


Figure 7: Two-tier EtherCAT based communication network.

The network as installed in the demonstrator consists of 1 EC slave for the time reference – this is integrated into the Zynq – and 4 EC slaves for the power racks, each of which is connected to 12 FSO links for a total of 48 cells (Figure 7). The achieved control cycle time is 100 μ s, including 20 μ s of preprocessing and 58 μ s of main control algorithm processing time and a maximum steady state jitter of 100 ns. Figure 8b) shows the minimal cabinet-to-cabinet wiring, consisting of two EC and one auxiliary power supply cables only. Figure 8c) shows, the RJ45 cables distributing the signal to the IR links. All wiring is at ground potential and no optical fiber is used.

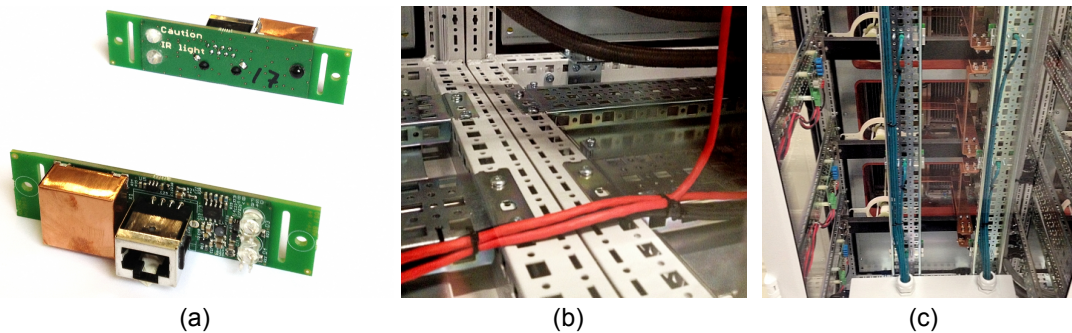


Figure 8: Photos of actual FSO boards (a), cabinet-to-cabinet wiring (b) and RJ45 cabling for signal distribution from EC slaves to each PEBBs FSO links (c).

2.5. Sensorless T_{junction} Measurement System

With regard to the total FIT (failure in time) rates, modular systems will theoretically always have a lower reliability than integrated solutions due to the higher part count. This can partly be compensated by introducing redundancy, which is possible with MMC type topologies. Advanced diagnostics methods applied to each module will further help to make best use of this redundancy. For that purpose, a sensorless IGBT junction temperature (T_j) measurement method has been developed. The method uses the gate voltage V_{GE} and the collector current I_c values available on the gate unit to extract the actual T_j at each switching operation and is based on the temperature dependency of the Miller-plateau length at turn-off [16] (Figure 9a). This length is, however, also dependent on the actual collector current I_c , which is taken into account using the current dependent voltage drop across the auxiliary and main emitter terminals [17] (Figure 9b). The achieved accuracy, within the nominal measurement range around $T_j = 125^\circ\text{C}$, is $\pm 5^\circ\text{C}$.

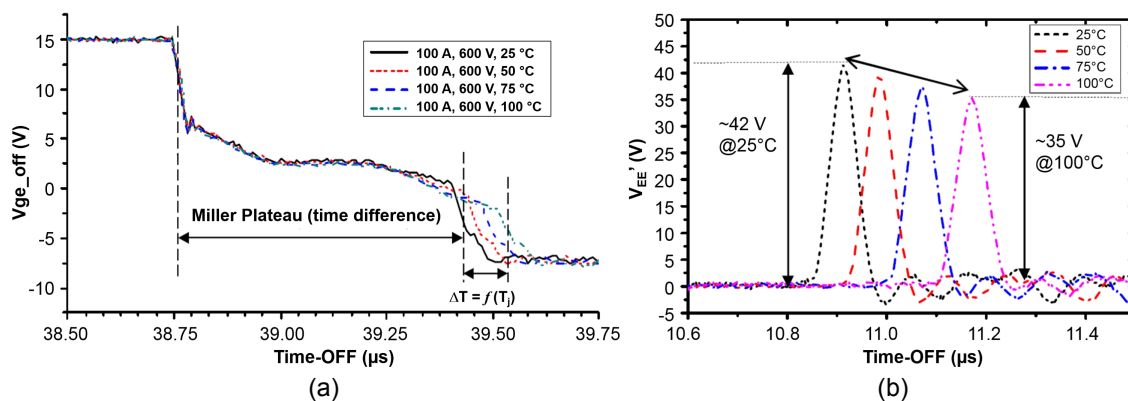


Figure 9: T_j measurement principle based on V_{GE} Miller plateau length (a) and I_c measurement based on voltage drop across auxiliary and main emitter terminals (b).

3. Demonstrator Converter

In order to prove that the developed technologies also work under real conditions, a full scale medium voltage ($V_{DC,max} = 11$ kV) converter was built (Figure 1a). As earlier mentioned, an MMC topology was chosen with a total of 12 cells per branch. The test setup consists of two single phases in back-to-back configuration, thus resulting in a total of 48 cells. Currently, a natural balancing, carrier based PWM control scheme is applied [19].

The modular technologies developed proved to be of great advantage already during commissioning of the demonstrator: The rail system in the rack and the pluggability of all PEBB interfaces allowed easy population of the converter cabinets with the 24 PEBBs (Figure 10). Thanks to the auxiliary power supply, the full converter control and communication was functional without connecting to the main power and all software configuration could be done offline under safe low voltage conditions.

The demonstrator was successfully tested including hot swap at a DC-link voltage of 3.3 kV and output power of 550 kW (single phase). The hot swap sequence consists of following steps: switch to reduced number of levels, closing the rack-mounted bypass switch, pulling-out the PEBB, re-entering a PEBB, opening the bypass switch and going back to the full number of levels (Figure 11).



Figure 10: Two PEBBs (a) and cabinets slots for two PEBBs with connecting elements (b).

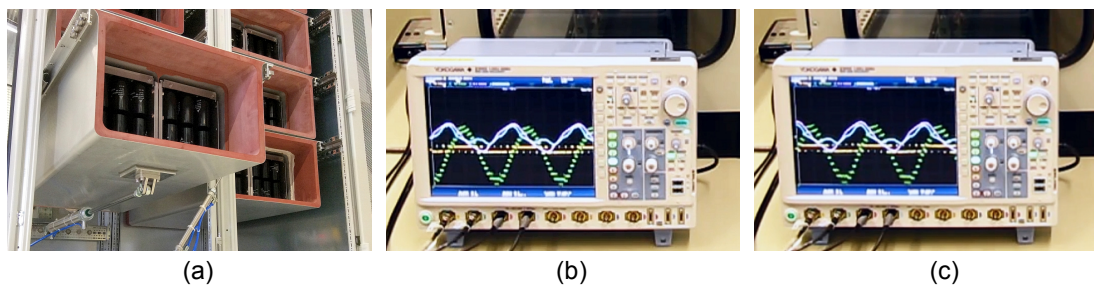


Figure 11: Close-up of a pulled-out module (a) and scope curves showing the 13 levels in normal operation (b) and the 11 levels when one module (consisting of two cells) is removed (c).

4. Conclusion

Integration technologies for modular medium voltage converters were developed and a full scale MV modular multi-level concept converter was built to demonstrate the benefits of these technologies. They were developed with regard to three key aspects of modularity: *scalability*, *configurability* and *pluggability* and through this already proved advantageous during the commissioning of the converter. Main benefits are the possibility of communicating with the modules in offline mode (disconnected from main power) to easily configure software, the

pluggability of the power modules without screwing and cable connection, and the scaling and configuring of the converter control hard- and software to match different converter setups. Finally, the combination of all technologies enabled the hot swap functionality, where power modules can be replaced during converter operation.

References

- [1] Ch. Huang, A. Kusiak, "Modularity in design of products and systems," *IEEE Trans. on Systems, Man and Cybernetics – Part A*, vol. 28, no. 1, pp. 66-77, January 1998.
- [2] Ch. Schäfer, "On the modularity of manufacturing systems," *IEEE Industrial Electronics Magazine*, pp. 22-27, fall, 2007.
- [3] Ch.H. Fine, "Are you modular or integral? Be sure your supply chain knows," *Strategy and Business Magazine*, issue 39, summer 2005.
- [4] R. Marquart, A. Lesnicar, and J. Hildinger, "Modulares Stromrichterkonzept für Netzkupplungsanwendungen bei hohen Spannungen," in *ETG-Fachtagung*, Bad Nauheim, Germany, 2002.
- [5] B. Wunsch, J. Bradshaw, I. Stevanovic, F. Canales, W. Van-der-Merwe, D. Cottet, "Inductive power transfer for auxiliary power of medium voltage converters," *Proc. APEC 2015 Conference*, Charlotte NC, USA, March 15-19, 2015.
- [6] C.-S. Wang, G. A. Covic, and O. H. Stielau, "Power transfer capability and bifurcation phenomena of loosely coupled inductive power transfer systems," *IEEE Trans. Ind. Electron.*, vol. 51, Feb. 2004.
- [7] W. Zhang, S. Wong, C. K. Tse, and Q. Chen, "Design for Efficiency Optimization and Voltage Controllability of Series-Series Compensated Inductive Power Transfer Systems," *IEEE Trans. Power Electron.*, vol. 29, no. 1, pp. 191–200, Jan. 2014 .
- [8] I. Mudawar, "Assessment of high-heat-flux thermal management schemes," *Proc. IEEE InterSociety Conf. on Thermal Phenomena*, 2000.
- [9] F. Agostini, T. Gradingner, D. Cottet, "Compact Gravity Driven and Capillary-Sized Thermosyphon Loop for Power Electronics Cooling", *J. Thermal Sci. Eng. Appl.*, vol. 6, no. 3, September 2014.
- [10] F. Agostini, T. Gradingner, "L-shaped thermosyphon loop with vertical evaporator for power electronics cooling", *IHTC15-8546/EEC-H-223, 15th Intl. Heat Transfer Conf.*, Kyoto, Japan, 2014.
- [11] T. Gradingner, F. Agostini, D. Cottet, "Two-phase cooling of hot-swappable modular converters," *Proc. Intl. Conf. for Power Electronics, Intelligent Motion, Renewable energy and Energy Management, PCIM Europe*, Nuremberg, 20-22 May, 2014.
- [12] M. Steiner, H. Reinold: "Medium frequency topology in railway applications", *Proc. of the European Conference on Power Electronics and Applications*, Aalborg, Denmark, pp. 1 – 10, 2007.
- [13] R. Velthuis, W. Gerig, T. Gradingner, F. Agostini, D. Cottet, "One-piece solid insulation for electrical enclosures," in *Kunststoffe International*, no. 12, 2014, pp- 31-34.
- [14] D. Orfanus, R. Indergaard, "Recovery of distributed clock in EtherCAT with redundancy for time-drift sensitive applications," *Proc. of the IEEE 19th Conference on Emerging Technologies Factory Automation (ETFA)*, Barcelona, Spain, September 16-19, 2014, pp. 1–4.
- [15] D. Orfanus, R. Indergaard, G. Prytz, and T. Wien, "EtherCAT-based platform for distributed control in high-performance industrial applications," *Proc. of the IEEE 18th Conference on Emerging Technologies Factory Automation (ETFA)*, Cagliari, Italy, September 2013, pp. 1–8.
- [16] V. Sundaramoorthy, E. Bianda, R. Bloch, I. Nistor, G. Knapp, A. Heinemann, "Online estimation of IGBT junction temperature (Tj) using gate emitter voltage (Vge) at turn-off," *Proc. of the European Conference on Power Electronics and Applications*, Lille, France, 3-5 Sept. 2013.
- [17] V. Sundaramoorthy, E. Bianda, R. Bloch, F. Zurfluh, "Simultaneous online estimation of junction temperature and current of IGBTs using emitter-auxiliary emitter parasitic inductance," *Proc. Intl. Conf. for Power Electronics, Intelligent Motion, Renewable energy and Energy Management, PCIM Europe*, Nuremberg, 20-22 May, 2014.
- [18] G. Riedel, N. Oikonomou, D. Cottet, R. Schmidt, "Active lifetime extension – demonstrated for voltage source converters," *Proc. IEEE 26th Convention of Electrical and electronics Engineers in Israel, IEEEI*, Eilat, Israel, 17-20 Nov. 2010.
- [19] W. van der Merwe, L. Stepanova, "Analysis of the 5-Cell Single Phase MMC Natural Balancing Mechanism," *Proc. ECCE 2014 Conference*, Pittsburgh, USA, pp. 3416–3423, 14-18 Sept. 2014.